

pubs.acs.org/JACS Article

# Reactivity of Cyclic and Linear Alkyl Carbonates with Reactive Oxygen Species

Bernardine L. D. Rinkel, Rohith Srinivaas Mohanakrishnan, Jaeheon Lee, Kristin A. Persson, and Bryan D. McCloskey\*



Cite This: https://doi.org/10.1021/jacs.5c12089



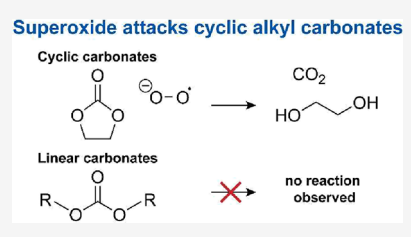
**ACCESS** I

III Metrics & More

Article Recommendations

s Supporting Information

ABSTRACT: Electrolyte decomposition at the positive and negative electrodes remains a major challenge to improving lithium-ion battery lifetime. At the positive electrode, chemical oxidation of alkyl carbonate solvents by reactive lattice oxygen species (ROS) has emerged as a key degradation pathway, but the specific reactivity of different solvents toward various ROS and the underlying mechanisms remain unclear. Here, we examine the reactivity of four widely used alkyl carbonates (EC, DMC, EMC, and DEC) with singlet oxygen, peroxide, and superoxide. Gas evolution measurements were used to assess the extent of reactions, and mass spectrometry and NMR spectroscopy identified the resulting



products to elucidate reaction pathways. EC was reactive toward all three ROS, with the highest reactivity for superoxide, followed by peroxide and singlet oxygen. Identified products enabled a proposed mechanism for EC oxidation, supported by DFT calculations. In contrast, the linear carbonates (DMC, EMC, and DEC) exhibited minimal reactivity under the same conditions, indicating greater resistance to ROS-induced oxidation. These findings suggest that reducing the EC content in electrolytes could mitigate degradation, particularly in next-generation cathodes with extensive oxygen redox that generate more ROS. This work provides mechanistic insight into solvent—ROS interactions and offers guidelines for designing more stable electrolytes for advanced lithium-ion batteries.

#### INTRODUCTION

The decomposition of the electrolyte solution at both the negative and positive electrodes is a major factor contributing to the capacity fade of lithium-ion batteries, ultimately limiting their lifetime. Research has largely focused on understanding the electrolyte decomposition reactions occurring at the negative electrode, as these reactions are essential for battery functioning. Research from the past decade has also demonstrated that electrolyte decomposition does occur at the positive electrode, as evidenced by observed gas evolution and the identification of decomposition products originating from reactivity at the positive electrode. 1—4

While this electrolyte decomposition at the positive electrode has predominantly been attributed to electrochemical oxidation reactions,  $^{5-7}$  recent work has led to the proposal of an alternative mechanism, in which reactive lattice oxygen species chemically oxidize the carbonate solvent. Here, the electrolyte solvent—typically a mixture of linear and cyclic alkyl carbonates—is attacked by so-called reactive oxygen species (ROS). This mechanism is supported by the observation of coupled  $CO_2$  and  $O_2$  evolution from a variety of positive electrode materials, such as layered transition metal oxides (i.e.,  $\text{LiNi}_x \text{Mn}_y \text{Co}_z O_2$ ;  $\text{NMC}_x yz$ ),  $^{1,2,4,8,9}_{1,2,4,8,9}$  as well as lithium-rich layered (i.e.,  $\text{Li}_{1+x} \text{M}_{1-y} O_2$ ; M = Ni, Mn,  $\text{Co})^{10,11}$  and disordered transition metal oxides (DRX; e.g.,  $\text{Li}_{1,2} \text{Mn}_{0,4} \text{Ti}_{0,4} O_2$ ),  $^{12,13}_{1,2,13}$  at potentials well below the reported

oxidative stability limit of the electrolyte solution (>5.5 V vs  $\text{Li/Li}^+$ ). <sup>14,15</sup>

The exact nature of the reactive lattice oxygen species remains unclear. The evolution of molecular oxygen  $(O_2)$  from these transition metal oxides positive electrode materials implies the (complete) oxidation of lattice oxygen  $(O^{2-})$ . However, the exact pathway by which lattice oxygen is oxidized and released, and the nature of the intermediate reactive oxygen species in the lattice, are still unclear. Emission spectroscopy has shown that the molecular oxygen is released from the transition metal oxide in the singlet excited state (1O2),8 which is more reactive than the triplet ground state  $(^{3}O_{2})$ . The presence of peroxo-like (O-O) dimers in these materials has been identified through various X-ray based techniques, although the existence of these species remains heavily debated. 18 Ab initio modeling suggests that oxide ion radicals (O'-) may form, which may subsequently combine to generate peroxide ions or evolve O2 at the transition metal oxide surface. 19 Thus, singlet oxygen, peroxide and superoxide

Received: July 15, 2025 Revised: October 17, 2025 Accepted: October 21, 2025



could all be relevant reactive lattice oxygen species responsible for the chemical oxidation of the electrolyte solvent.

Studies on Li-O2 batteries, where ROS such as superoxide and peroxide are generated, have demonstrated that alkyl carbonate solvents are incompatible with these ROS.2 However, few studies have explored the underlying mechanisms of this reactivity. Density functional theory (DFT) calculations have investigated the reactivity of propylene carbonate (PC) with peroxide<sup>24</sup> and superoxide,<sup>2</sup> proposed possible reaction mechanisms. Experimental work has identified the discharge products that form in a Li-O2 cell using PC as the electrolyte solvent, and used these products to propose a mechanism where PC is oxidized by superoxide.<sup>21</sup> Gas evolution and NMR studies have shown that ethylene carbonate (EC) reacts with singlet oxygen to form CO<sub>2</sub> and  $\rm H_2O$ , whereas dimethyl carbonate (DMC) appears unreactive toward singlet oxygen.  $^{4,26}$  However, DFT studies comparing the reactivity of EC with singlet oxygen, peroxide and superoxide species suggest that singlet oxygen is not a likely culprit; instead peroxide species are more likely to be responsible for carbonate oxidation.<sup>27</sup>

Despite these observations, our understanding of the reactivity of alkyl carbonate solvents with ROS remains limited. Specifically, it is unclear which ROS the alkyl carbonates are most reactive toward, whether all carbonate solvents display similar reactivity, and the mechanisms by which these reactions proceed—all of which makes it challenging to assess and mitigate the impact of electrolyte decomposition on the battery's lifetime.

In this work, the reactivity of both cyclic (EC) and linear alkyl carbonate solvents (DMC, EMC and DEC) with the reactive oxygen species singlet oxygen ( ${}^{1}O_{2}$ ), peroxide ( ${}^{2}O_{2}$ ), and superoxide (O2-) was investigated. Gas evolution measurements were used to determine the presence and extent of reactions between the solvents and ROS. The resulting gaseous and soluble reaction products were characterized by mass spectrometry (MS) and NMR spectroscopy, respectively, to gain insights into the reaction pathway. EC was found to be reactive toward all three ROS, with significantly greater reactivity toward superoxide than toward peroxide and singlet oxygen. The resulting products were used to propose a mechanism for the chemical oxidation of EC, which is supported by density functional theory (DFT) calculations. In contrast, the linear alkyl carbonates, DMC, EMC, and DEC, showed minimal reactivity under the conditions explored, suggesting that the linear alkyl carbonate solvents possess a greater inherent resistance to chemical oxidation by ROS.

# **■ EXPERIMENTAL SECTION**

The chemical reactivity between ROS and alkyl carbonates was assessed by monitoring gas evolution during the reaction, identifying and quantifying the gaseous decomposition products using mass spectrometry, and characterizing soluble products by NMR spectroscopy. Five commonly used alkyl carbonate solvents were selected: two cyclic carbonates, ethylene carbonate (EC; Gotion) and propylene carbonate (PC; 99.7%, Sigma-Aldrich) and three linear carbonate, dimethyl carbonate (DMC; Gotion), ethyl methyl carbonate (EMC; Gotion) and diethyl carbonate (DEC, Gotion) were used as received. Two electrolyte additives, vinylene carbonate (VC; Gotion) and fluoroethylene carbonate (FEC; Gotion) were also included and used as received. To closer resemble practical electrolyte solutions, a mixture of EC and DMC (1:1 v/v) and a 1 M LiPF<sub>6</sub> (Gotion) in EC:DMC (1:1 v/v) were also evaluated.

**Singlet Oxygen.** Singlet oxygen was produced in a carbonate solution using a previously reported method:  $^{4,26}$   $^{1}\mathrm{O}_{2}$  was generated in triplet oxygen ( $^{3}\mathrm{O}_{2}$ ) saturated solutions of EC, DMC, EMC and DEC, by photoexcitation of  $^{3}\mathrm{O}_{2}$  to  $^{1}\mathrm{O}_{2}$  using Rose Bengal as a photosensitizer. Irradiating Rose Bengal with light at 525 nm results in the formation of a triplet state of Rose Bengal, which can then transfer energy to  $^{3}\mathrm{O}_{2}$  during a collision between Rose Bengal and  $^{3}\mathrm{O}_{2}$ , exciting  $^{3}\mathrm{O}_{2}$  to  $^{1}\mathrm{O}_{2}$ .

Rose Bengal salt (disodium salt, >95%, Sigma-Aldrich) was dried at 120  $^{\circ}$ C under dynamic vacuum for 72 h. Solutions of 100  $\mu$ M Rose Bengal in EC, DMC, EMC, and DEC were prepared in an argon-filled glovebox.

To detect the evolution of gaseous products resulting from the reaction between  $^1\mathrm{O}_2$  and the alkyl carbonates, a custom-made, three-neck glass vessel was used, which can be hermetically sealed and connected to a gas-handling/MS system, as described in our previous work. The glass vessel was filled with 2 mL of the Rose Bengal/carbonate solution and a magnetic stir bar was added for convective mixing during irradiation of the solution. The glass vessel was sealed to create an air and moisture tight container, and transferred out of the glovebox. Oxygen gas (>99.993%, UHP T, Praxair) was bubbled through the solution for 10 min to ensure the Rose Bengal/carbonate solution was saturated with oxygen.

The glass vial containing the Rose Bengal/carbonate solution was placed on a magnetic stirrer between four LEDs and irradiated with light at 525 nm. A current of 400 mA was applied to the LEDs for 24 h. The extended irradiation of the Rose Bengal/carbonate solution for 24 h may lead to some degree of photobleaching of Rose Bengal, and thus the generation of singlet oxygen may become less efficient.

Due to the high melting point of EC, all experiments (including those with the linear alkyl carbonates) were performed at 50 °C.

After irradiation, the vessel headspace ( $\sim$ 10 mL) was purged with 2 mL of argon every 4 min to sweep any evolved gases to the mass spectrometer, and 100  $\mu$ L of the Rose Bengal/carbonate solution was taken for analysis by solution NMR.

**Peroxide.** The reactivity of alkyl carbonate solvents with peroxide was studied by adding lithium peroxide to each of the four carbonates. Lithium peroxide (Li $_2$ O $_2$ ; 95%, Alfa Aesar) was dried at 120 °C under dynamic vacuum for 72 h. Solutions of 100 mM lithium peroxide in EC, DMC, EMC, and DEC were prepared in an argon-filled glovebox. Since the reaction between the peroxide and the alkyl carbonates was suspected to begin immediately upon contact, solutions of lithium peroxide in carbonate (2 mL) were directly prepared in the glass vessel described above. The vessel was promptly sealed and transferred out of the glovebox and directly connected to the gashandling/MS system within 2 min of preparing the peroxide solution, to maximize the capture of evolved gases; however, despite these precautions, some loss of initially evolved gases cannot be ruled out

Samples for NMR analysis were prepared in a similar manner in a HDPE vial equipped with a magnetic stir bar and the peroxide/carbonate mixture was left stirring at 50 °C for 72 h, after which 100  $\mu$ L of the peroxide/carbonate solutions was taken for analysis by solution NMR.

To improve the solubility of lithium peroxide in alkyl carbonates, the above experiments were repeated with the addition of a crown ether. Equimolar amounts of 12-crown-4 (1,4,7,10-tetraoxacyclododecane, 98%, Sigma-Aldrich), were added to the peroxide/carbonate solutions.

**Superoxide.** The reactivity of the carbonate solvents with superoxide was investigated by adding potassium superoxide to each of the alkyl carbonates. Potassium superoxide ( $KO_2$ , Acros Organics) was used as received. Solutions of 100 mM potassium superoxide were prepared in individual solvents, EC, PC, DMC, EMC, DEC, VC, and FEC, in solvent mixtures, EC/DMC (50:50 v/v), and EC/EMC (50:50 v/v), and in an electrolyte solution of 1 M LiPF<sub>6</sub> (Gotion) in EC/DMC (50:50 v/v).

The experiments were performed as described above for the peroxide reactions. The reaction between carbonates and superoxide was noticeably faster than that observed for peroxide (see main text), hence NMR samples were taken after 15 min, 2, 12, 24, 48, 72, and 96

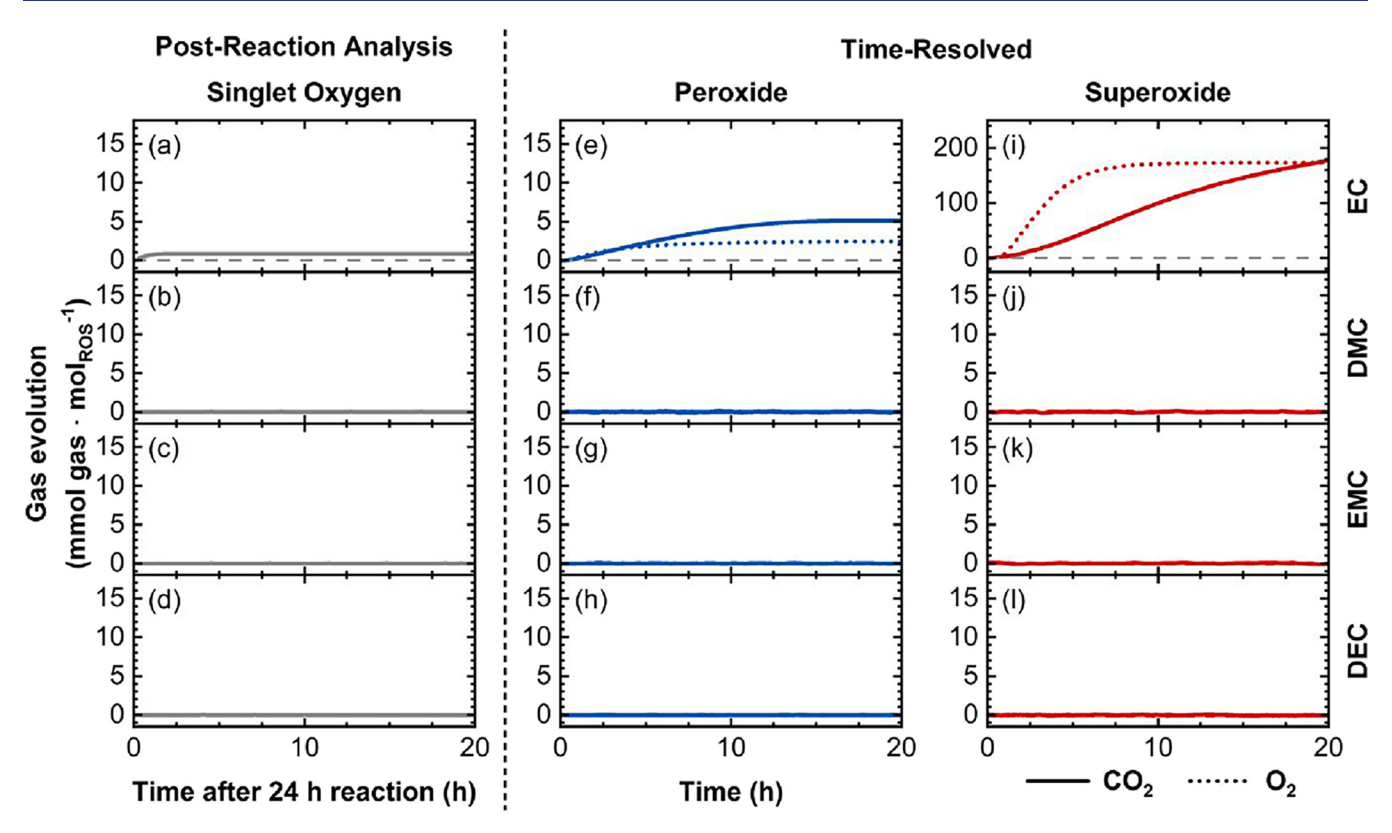


**Figure 1.** CO<sub>2</sub> (solid) and O<sub>2</sub> (dotted) evolution during the reaction of singlet oxygen (a–d), lithium peroxide (e–h) and potassium superoxide (i–l) with four different alkyl carbonates: ethylene carbonate (EC; top row), dimethyl carbonate (DMC; second row), ethyl methyl carbonate (EMC; third row) and diethyl carbonate (DEC; bottom row). Peroxide and superoxide were used at a concentration of 100 mM, while singlet oxygen was used at 1.5 mM, limited by the solubility of molecular oxygen in the carbonate solvents. The gas evolution is normalized to the initial amount of ROS (mmol<sub>gas</sub>/mol<sub>ROS</sub>). All experiments were performed without the addition of a crown ether. Note the different *y*-axis scale for panel (i), which shows the reaction between EC and potassium superoxide. For singlet oxygen, the time axis represents the time at which gases were analyzed after a 24 h reaction, rather than the progression of the reaction itself.

h to capture the full range of decomposition products and intermediates. To improve the solubility of potassium superoxide in the alkyl carbonates, particularly the linear ones, the above experiments were repeated with the addition of equimolar amounts of 18-crown-6 (1,4,7,10,13,16-hexaoxacyclooctadecane,  $\geq$ 99.0%, Sigma-Aldrich).

To quantify any unreacted potassium superoxide remaining in solution after a 24 h reaction period, water (0.5 mL; argon-sparged) was injected into the reaction vessel to quench any unreacted superoxide. The oxygen evolved from this reaction  $(O_2^- + H_2O \rightarrow OH^- + \frac{1}{2}O_2)$ , was used to back-calculate the quantity of unreacted superoxide remaining in the carbonate solution.

**Gas Measurements.** The gases evolved from the reaction between the ROS and alkyl carbonate solvents were characterized and quantified using a custom-built system that handles gas flow from the glass vessel to a MS gas analyzer, which has been described previously.  $^{13,29,30}$  Argon (ultrahigh purity, Linde gas) was used as the carrier gas, unless otherwise stated. The glass vessel headspace ( $\sim$ 10 mL) was purged with 2 mL of argon every 15 min (or every 4 min for the singlet oxygen experiments) and any accumulated gases were swept to the mass spectrometer chamber for analysis. The mass spectrometer was calibrated for  $O_2$  (research grade, Linde) and  $CO_2$  (>99.9%, Linde), allowing for the conversion of the ion current to partial pressure for  $O_2$  and  $CO_2$ , which could then be used to quantify the gas formation using the ideal gas law (temperature and volume are known).

**Solution NMR.** Sample of carbonates after reaction with reactive oxygen species (0.1 mL) were diluted in DMSO- $d_6$  (0.5 mL, Aldrich, 99.9 atom % D, 99% CP), after which the solution was transferred to an NMR tube.

One-dimensional  $^1\text{H}$  NMR spectra and two-dimensional  $^1\text{H}-^1\text{H}$  correlation spectroscopy (COSY) NMR spectra were recorded on a Bruker AVANCE III HD 14.1 T ( $\omega_{1\text{H}}=600$  MHz) spectrometer using a BB Prodigy CryoProbe.  $^1\text{H}$  spectra were internally referenced to DMSO- $d_6$  at 2.50 ppm ( $\delta^1\text{H}$ ).

Density Functional Theory. Molecular density functional theory (DFT) calculations were performed to aid in elucidating the reaction mechanism EC and potassium superoxide. DFT calculations were performed using PySCF<sup>31</sup> to enable GPU acceleration for geometry optimization. To obtain the geometries of the reactants, products, and transition states, calculations were performed using the w97M-V range separated meta-Generalized Gradient approximation density functional with def2-svpd basis set.<sup>33</sup> Solvent effects were modeled implicitly using the solvent model with density (SMD),<sup>34</sup> with previously reported parameters for ethylene carbonate,<sup>35</sup> including a dielectric constant of 90.32 Nudged Elastic Band (NEB) Calculations<sup>36</sup> with Image-Dependent Pair Potential(IDPP)<sup>37</sup> performed with 11 images between the reactant and product geometries to obtain the initial approximation of the transition state geometry. This approximation was further optimized using Sella<sup>38</sup> to obtain a structure with exactly one imaginary frequency. The optimized transition state was verified by performing intrinsic reaction coordinate (IRC)<sup>39</sup> calculations to confirm its connection to the reactant and product geometries. Both the reactant and product geometries were confirmed to have zero imaginary frequencies.

To obtain accurate thermochemical data for the optimized geometries, frequency calculations were performed using the w97M-V range separated meta-generalized gradient approximation (meta-GGA) functional<sup>32</sup> with the def2-TZVPPD basis set.<sup>33</sup> All thermochemical calculations were performed using the Q-Chem version 6 electronic structure code,<sup>40</sup> employing the quasi-rigid rotor

Table 1. Quantification of CO<sub>2</sub> and O<sub>2</sub> Evolved from Reaction between the Reactive Oxygen Species, Singlet Oxygen, Peroxide, and Superoxide with EC, DMC, EMC, and DEC<sup>a</sup>

solvent	singlet $O_2$ ( $^1O_2$ )		peroxide (O <sub>2</sub> <sup>2-</sup> )		superoxide (O <sub>2</sub> <sup>-</sup> )	
gas	CO <sub>2</sub>	O <sub>2</sub>	CO <sub>2</sub>	O <sub>2</sub>	CO <sub>2</sub>	$O_2$
	$\mathrm{mmol}_{\mathrm{gas}}/\mathrm{mol}_{\mathrm{ROS}}$		$\mathrm{mmol}_{\mathrm{gas}}/\mathrm{mol}_{\mathrm{ROS}}$		$\mathrm{mmol}_{\mathrm{gas}}/\mathrm{mol}_{\mathrm{ROS}}$	
EC	0.9		5.1	2.4	190.8	174.2
PC					7.4	59.3
DMC	0.0		0.0		0.0	
EMC	0.0		0.0		0.0	
DEC	0.0		0.0		0.0	
EC/DMC					206.1	172.4
1 M LiPF <sub>6</sub> in EC/DMC					162.3	209.2

<sup>&</sup>quot;aAmount of gas evolved after 24 hours, normalized to the initial amount of ROS added (mmol<sub>gas</sub>/mol<sub>ROS</sub>). All values correspond to experiments performed without the addition of a crown ether.

harmonic oscillator (q-RRHO) approach<sup>41</sup> to properly account for frequency vibrational modes.

#### RESULTS

Assessing Reactivity between Reactive Oxygen Species and Alkyl Carbonates and Analysis of Gaseous **Products through Mass Spectrometry.** The reactivity of singlet oxygen, peroxide, and superoxide with alkyl carbonate solvents was initially assessed by characterizing and quantifying the gaseous decomposition products formed upon reaction. Four commonly used carbonate solvents were investigated: the cyclic carbonate ethylene carbonate (EC), and three linear carbonates dimethyl carbonate (DMC), ethyl methyl carbonate (EMC) and diethyl carbonate (DEC). For peroxide and superoxide, a concentration of 100 mM was used, which exceeds the estimated O2 concentration in the electrolyte solution (~10 mM) that would be evolved from NMC811 electrodes charged to 4.4 V, assuming  $O_2$  loss of ~25  $\mu$ mol/  $g_{NMC}$  and an electrolyte/electrode ratio of ~2.5 mL/ $g_{NMC}$ . For singlet oxygen, the concentration was limited by the solubility of molecular oxygen in the carbonate solvents, resulting in a lower concentration of 1.5 mM being used.<sup>33</sup> The gas evolution from all reactions presented below is normalized to the ROS concentration to allow for a direct comparison of reactivity between the different species.

Singlet Oxygen. To establish the reactivity between singlet oxygen ( $^{1}O_{2}$ ) and alkyl carbonate solvents,  $^{1}O_{2}$  was produced in four carbonate solutions, using a previously reported method:  $^{4,26}$  Rose Bengal was used as a photosensitizer to generate  $^{1}O_{2}$  in triplet oxygen ( $^{3}O_{2}$ )-saturated solutions of ethylene carbonate (EC), dimethyl carbonate (DMC), ethyl methyl carbonate (EMC) and diethyl carbonate (DEC), by irradiating the solution with light at 525 nm. To confirm that  $^{1}O_{2}$  was indeed produced by the photosensitizer, a solution of dimethyl anthracene (DMA) and Rose Bengal in EC was irradiated for 2 h, and analysis by solution NMR indicated the formation of the endoperoxide of DMA, confirming that  $^{1}O_{2}$  was generated (Figure S1).  $^{34}$ 

As this reaction requires an  $O_2$  atmosphere, it could not be performed while directly connected to the mass spectrometer, as this would saturate the MS filament. An attempt to perform operando gas measurements using 10%  $O_2$  in Ar as a carrier gas did not result in the formation of any detectable gaseous products (Figure S2), possibly due to inadequate  $O_2$  saturation of the solvent from the carrier gas. Instead, the reaction was performed under a pure oxygen atmosphere for 24 h, after

which any gases accumulated in the vessel headspace were characterized and quantified by mass spectrometry.

The gaseous products evolved during the 24 h reaction between singlet oxygen and the four carbonate solvents are shown in Figure 1a-d, and quantification of the gases is given in Table 1. Note that for these experiments with singlet oxygen, the x-axis represents the time required to analyze the gases after the reaction occurred, rather than the progression of the reaction. The reaction between EC and singlet oxygen resulted in a small amount of CO<sub>2</sub> being formed (~0.86 mmol<sub>CO2</sub>/mol<sub>ROS</sub>; Figure 1a). Isotopic labeling experiments with <sup>18</sup>O<sub>2</sub> further confirmed that the CO<sub>2</sub> generated in the reaction of EC with singlet oxygen originates from molecular oxygen (Figure S3). In contrast, no gaseous products could be detected or the reaction of singlet oxygen with each of the three linear alkyl carbonates (Figure 1b-d). The solubility of CO<sub>2</sub> in all four alkyl carbonate solvents is comparable and therefore cannot account for the observed differences in CO2 evolution.<sup>35</sup> These results are consistent with previous studies on the reactivity of singlet oxygen with EC and DMC.<sup>26</sup>

*Peroxide.* To investigate the reactivity between peroxide and the four alkyl carbonate solvents, lithium peroxide (Li<sub>2</sub>O<sub>2</sub>) was used as a chemical source of peroxide. The gaseous products formed during the reaction were directly monitored using mass spectrometry (Figure 1e–h). For EC, a modest amount of  $CO_2$  (~5.1 mmol<sub>CO2</sub>/mol<sub>ROS</sub>) is formed (Figure 1e), suggesting a greater reactivity with peroxide than with singlet oxygen. Additionally, a small amount of  $O_2$  evolved during this reaction. No  $CO_2$  could be detected for the reaction between lithium peroxide and the three linear carbonates (Figure 1f–h), similar to what was observed for the reaction with singlet oxygen. The detection limit of the mass spectrometer was estimated to be ~5.5  $\times$  10<sup>-14</sup> mol<sub>CO2</sub>/L, corresponding to a maximum of ~9  $\times$  10<sup>-15</sup> moles for possible undetected  $CO_2$  formation for the linear alkyl carbonates.

Due to the low solubility of  $\text{Li}_2\text{O}_2$  in alkyl carbonate solvents, the measurements were repeated with the addition of the crown ether, 12-crown-4, to improve  $\text{Li}_2\text{O}_2$  solubility (Figure S4e-h). Similar results were obtained upon the addition of the crown ether: the reaction with EC gave  $\sim$ 4 mmol $_{\text{CO}_2}/\text{mol}_{\text{ROS}}$  (cf.  $\sim$ 5 mmol $_{\text{CO}_2}/\text{mol}_{\text{ROS}}$  without the crown ether), and gas evolution remained undetectable for the linear alkyl carbonates. It is worth noting that in the presence of the crown ether, the final gas concentrations were reached within 1 h (cf. 10 h without the crown ether), suggesting that the reaction is accelerated, but not increased in extent, by the

enhanced availability of the peroxide anion due to cation complexation.

Superoxide. To explore the reactivity of superoxide with alkyl carbonate solvents, potassium superoxide (KO<sub>2</sub>) was used as a chemical source of superoxide, and the resulting evolution of gaseous products is shown in Figure 1i–l. For EC, the reaction resulted in the evolution of both CO<sub>2</sub> and O<sub>2</sub> (~200 mmol<sub>CO2</sub>/mol<sub>ROS</sub> and ~ 200 mmol<sub>O2</sub>/mol<sub>ROS</sub>, respectively), with a substantially greater amount of CO<sub>2</sub> produced compared to reactions with singlet oxygen or peroxide (Figure 1i; note the change in *y*-axis scale compared to all other panels). In contrast, no CO<sub>2</sub> could be detected for the linear carbonates over 24 h of reaction (Figure 1j–l), suggesting that these compounds are mostly unreactive toward superoxide on this time scale (~day).

To assess whether the high  $KO_2$  concentration used in our initial experiments influenced the observed reactivity, we repeated the reaction of  $KO_2$  with EC at two additional concentrations (10 and 1.5 mM), in addition to the original 100 mM. For all three concentrations, the amounts of  $CO_2$  and  $O_2$  when normalized per mole of reactive oxygen, were comparable (Figure S5). These results indicate that the greater reactivity observed for  $KO_2$  compared to singlet oxygen is not due to the higher concentration used.

To confirm that  $KO_2$  remained unreacted in the linear alkyl carbonates, a water titration was performed to quantify the remaining  $KO_2$  in the reaction mixtures: addition of water promotes the disproportionation of  $KO_2$  to  $H_2O_2$  and  $O_2$ , the latter of which can be quantified through mass spectrometry. For all three linear carbonate solvents, the water titration yielded the stoichiometric amount of  $O_2$  expected from the initial amount of  $KO_2$  (Section S3 and Figure S6b–d). This indicates that all  $KO_2$  remained unreacted in the presence of linear alkyl carbonate, thus further supporting that  $KO_2$  is unreactive toward the linear alkyl carbonates. This is in contrast with EC, where all  $KO_2$  had reacted after 24 h (Figure S6a).

The solubility of KO<sub>2</sub> in the carbonates, particularly the linear carbonates, was improved by adding a crown ether (18-crown-6) and the corresponding gas evolution results are shown in the Supporting Information (Figure S4i–l). For EC, the inclusion of the crown ether did not affect the overall reactivity ( $\sim$ 200 mmol<sub>CO2</sub>/mol<sub>ROS</sub> and  $\sim$ 230 mmol<sub>O2</sub>/mol<sub>ROS</sub> with the crown ether cf.  $\sim$ 200 mmol<sub>CO2</sub>/mol<sub>ROS</sub> and  $\sim$ 200 mmol<sub>O2</sub>/mol<sub>ROS</sub> without the crown ether), but significantly accelerated the reaction (1 vs >24 h), which is consistent with the observations for the peroxide experiments. For the linear alkyl carbonates, no CO<sub>2</sub> was detected even with the addition of a crown ether. However, a small amount of O<sub>2</sub> was detected, possibly due to trace protic impurities from the crown ether promoting the disproportionation of KO<sub>2</sub> to O<sub>2</sub> and H<sub>2</sub>O<sub>2</sub>.

Given that superoxide was found to be the most reactive ROS, its reactivity was further explored with additional solvents, additives, and more representative electrolyte solutions. Propylene carbonate (PC), another cyclic carbonate commonly used in electrolyte solutions, was first examined. As with EC, the reaction of PC with potassium superoxide resulted in the evolution of CO<sub>2</sub> and O<sub>2</sub> (Figure 2; blue trace). However, the reaction proceeded considerably slower, requiring almost 60 h for gas evolution to cease (Figure S7), indicating that PC is less reactive than EC toward superoxide under these conditions. Attempts to explore the reactivity between superoxide and the electrolyte additives VC and FEC

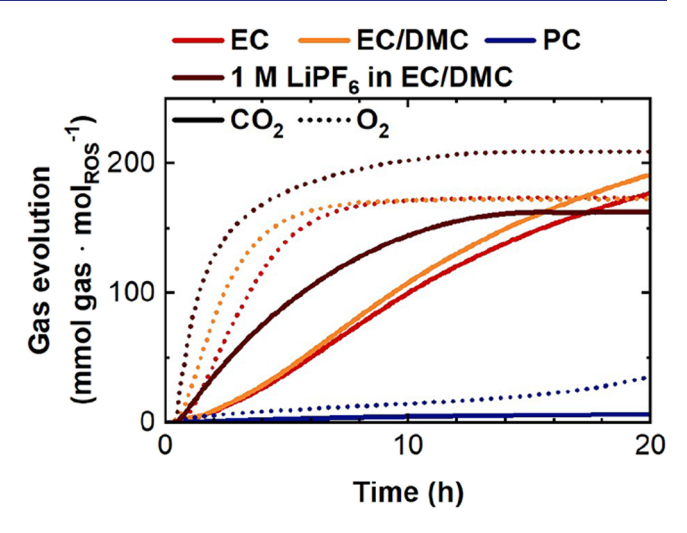


Figure 2.  $CO_2$  (solid lines) and  $O_2$  (dotted lines) evolution during the reaction of 100 mM potassium superoxide with EC (red), EC/DMC (1:1 v/v; orange), 1 M LiPF<sub>6</sub> in EC/DMC (1:1 v/v; brown) and PC (blue).

led to spontaneous and vigorous exothermic reactions immediately upon contact. Analysis of the headspace after combustion revealed  $\mathrm{CO}_2$  and  $\mathrm{O}_2$  as gaseous reaction products for FEC, and only  $\mathrm{CO}_2$  for VC (Figure S8).

To better mimic practical lithium-ion battery electrolytes, a mixture of cyclic and linear alkyl carbonates was also studied. The reaction of potassium superoxide with an EC/DMC mixture again resulted in the evolution of both CO<sub>2</sub> and O<sub>2</sub>, with a gas evolution rate comparable to that observed for a pure EC solution (Figure 2; orange vs red trace). The presence of DMC does not appear to significantly affect the reactivity of superoxide with EC.

Finally, the effect of a lithium salt on the reactivity of the carbonate solvent was investigated. The addition of 1 M LiPF<sub>6</sub> to the EC/DMC mixture again resulted in the evolution of both  $CO_2$  and  $O_2$ , with noticeably faster release of both gases (Figure 2; brown trace). The accelerated  $O_2$  evolution is attributed to the cation-induced disproportionation of potassium superoxide. This has been reported to be extensive in the presence of the lithium cation but is minimal for the much larger potassium cation. Similarly, the faster  $CO_2$  evolution may be due to lithium facilitating the dissolution of the superoxide salt, thereby enabling a more rapid reaction between the superoxide anion and EC.

Previous studies have shown that KO<sub>2</sub> can disproportionate to form singlet oxygen; however, this process is minimal in the presence of potassium cations and occurs predominantly with lithium, and to a lesser extent, sodium cations. 36,37 Disproportionation promoted by protic species also appears unlikely, as no H2O2 was detected in the reaction mixtures by NMR (see below). Therefore, significant singlet oxygen formation from KO2 disproportionation is unlikely under our experimental conditions. Furthermore, if singlet oxygen were the main reactive species, we would expect CO2 and O2 to evolve simultaneously during the reaction of KO<sub>2</sub> with EC, given the short lifetime of singlet oxygen in solution ( $\sim 10^{-6}$ s), 38 yet this is not observed (Figure 1i). This, combined with the minimal CO2 evolution observed upon direct generation of singlet oxygen (Figure 1a), suggests that singlet oxygen is not the primary contributor to carbonate solvent decomposition in our experiments.

Table 2. Summary of the Alkyl Carbonate Decomposition Products Identified by Solution-State NMR following Reaction with Different Reactive Oxygen Species<sup>a</sup>

ROS			Solvent	Assignment	Chemical shift (ppm)
			EC		4.48 (s)
			DMC		3.69 (s)
			EMC		$4.12 (q, {}^{3}J_{H-H} = 7.1 Hz);$
					3.69 (s);
					1.21 (t, ${}^{3}J_{\text{H-H}} = 7.1 \text{ Hz}$ )
			DEC		$4.10 (q, {}^{3}J_{H-H} = 7.0 Hz);$
					$1.20 \text{ (t, }^{3}J_{\text{H-H}} = 7.0 \text{ Hz)}$
$^{1}O_{2}$	$O_2^{2-}$	O <sub>2</sub> -			
			EC		
		✓		Glyoxal <sup>†</sup>	9.61 (s)
		✓		Glycolaldehyde <sup>†</sup>	9.41 (t, ${}^{3}J_{\text{H-H}} = 1.6 \text{ Hz}$ );
					$3.97 \text{ (t, }^{3}J_{\text{H-H}} = 1.6 \text{ Hz)}$
		✓		Formate	8.58 (s)
		✓		Potassium formate*	8.21 (s)
		<b>√</b>		Formic acid	8.18 (s)
		1		Potassium ethylene monocarbonate*	$4.13 \text{ (t, }^{3}J_{\text{H-H}} = 4.9 \text{ Hz);}$
		,		Peroxide-derivative of ethylene	$3.81 \text{ (t, }^{3}J_{\text{H-H}} = 4.9 \text{ Hz)}$
				monocarbonate*	,
	✓	<b>√</b>		Ethylene monocarbonate	$4.10 \text{ (t, }^{3}J_{\text{H-H}} = 4.8 \text{ Hz);}$
					$3.59 \text{ (t, }^{3}J_{\text{H-H}} = 4.8 \text{ Hz)}$
		✓		Polyethyleneoxide-like	$3.69 \text{ (t, }^{3}J_{\text{H-H}} = 5.1 \text{ Hz);}$
					$3.43 \text{ (t, }^{3}J_{\text{H-H}} = 5.1 \text{ Hz)}$
	✓	✓		Ethylene glycol	3.41 (s)
			DMC		
	✓	✓		Methanol	$4.10 (q, {}^{3}J_{H-H} = 5.5 Hz);$
					$3.17 \text{ (d, }^{3}J_{H-H} = 5.5 \text{ Hz)}$
	✓	✓		Dimethyl sulfone§	2.97 (s)
			EMC		
		✓		Potassium ethoxide*	3.61 (q, ${}^{3}J_{\text{H-H}} = 6.9 \text{ Hz}$ );
					$0.99 \text{ (t, }^{3}J_{\text{H-H}} = 6.9 \text{ Hz}$
	✓	✓		Ethanol	$3.44 (q, {}^{3}J_{H-H} = 6.8 Hz);$
					$1.06 \text{ (t, }^{3}J_{\text{H-H}} = 6.8 \text{ Hz}$
	✓	✓		Methanol	$4.10 \text{ (q, }^{3}J_{\text{H-H}} = 5.5 \text{ Hz)};$
		1			$3.17 \text{ (d, }^3J_{\text{H-H}} = 5.5 \text{ Hz)}$
		✓		Dimethyl sulfone§	2.97 (s)
			DEC		
		✓		Potassium ethoxide*	$3.61 (q, {}^{3}J_{H-H} = 6.9 Hz);$
					$0.99 \text{ (t, }^{3}J_{\text{H-H}} = 6.9 \text{ Hz}$
	✓	✓		Ethanol	$3.44 (q, {}^{3}J_{H-H} = 6.8 Hz);$
		1			$1.06 \text{ (t, }^{3}J_{\text{H-H}} = 6.8 \text{ Hz}$
		✓		Dimethyl sulfone§	2.97 (s)

"Chemical shifts (in ppm) and multiplicities with coupling constants (in Hz) are listed for each assigned species. A  $\checkmark$  indicates the species was present after that reaction. Transient species are denoted with a dagger (†) and tentative assignments are indicated with an asterisk (\*). Dimethyl sulfone (DMSO<sub>2</sub>; denoted with §) was observed for the linear carbonates after reaction with potassium superoxide; this species arises from the oxidation of DMSO during NMR sample preparation (see the main text for details).

These gas evolution measurements demonstrate that all three ROS are reactive toward cyclic alkyl carbonates, with superoxide displaying the highest reactivity and EC being the most reactive substrate. In contrast, the three ROS were unreactive toward the linear alkyl carbonates under the conditions tested.

Analysis of Soluble Products Formed through the Reaction of ROS with Alkyl Carbonates by NMR Spectroscopy. To identify any soluble decomposition products formed in the reaction between the alkyl carbonates and the three ROS,  $100~\mu\text{L}$  of the reaction mixture was diluted in DMSO- $d_6$  and characterized by  $^1\text{H}$  NMR spectroscopy. The results presented below are from experiments performed without the addition of a crown ether, as this can obscure NMR signals arising from reaction products and may also introduce impurities, further complicating analysis. The corresponding  $^1\text{H}$  NMR spectra obtained with a crown ether (Figures S9–S12) and a discussion of the spectral assignments

are given in the Supporting Information. In short, the assignments were made based on reported chemical shifts in the literature, as well as two-dimensional experiments (COSY) and J-coupling analysis. A list of the species observed in the carbonate solvents, their chemical shifts, and the conditions under which they were observed, is given in Table 2 and summarized below.

Cyclic Alkyl Carbonates. The  $^1$ H NMR spectrum of pristine EC (Figure 3d) shows one main signal arising from the solvent (EC; 4.48 ppm) and two minor signals arising from nondeuterated DMSO impurities in the DMSO- $d_6$  solvent (2.50 ppm), and trace quantities of water (3.33 ppm) originating from the deuterated NMR solvent (Figure S13). The reaction of EC with singlet oxygen results in a small increase in the water signal ( $\sim$ 2.5× by integration; Figure 3c), consistent with previous results. No other additional signals were observed, suggesting that the reaction with singlet oxygen only results in the formation of  $H_2O$  and  $CO_2$ .

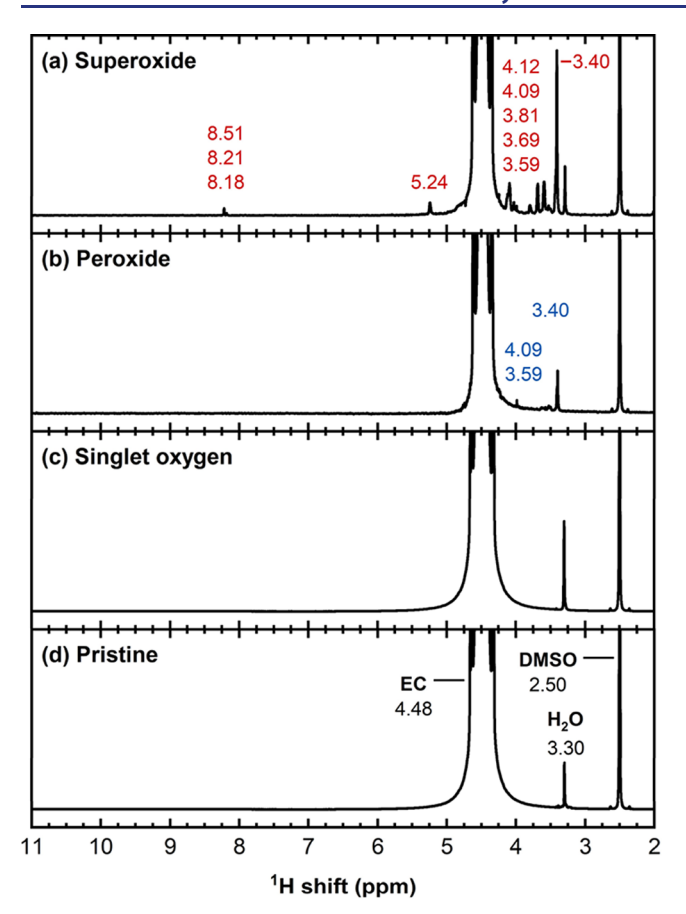


**Figure 3.** <sup>1</sup>H solution NMR spectra of ethylene carbonate (EC) after reaction with (a) potassium superoxide, (b) lithium peroxide and (c) singlet oxygen. (d) pristine EC. The signals of EC (4.48 ppm), dimethyl sulfoxide (2.50 ppm) and residual water (3.30 ppm) are annotated in black on the bottom panel. The chemical shifts in blue and red correspond to signals that appeared after a 24 h reaction with peroxide and superoxide, respectively.

In contrast, the reaction of EC with 100 mM lithium peroxide after 24 h yields three new signals (Figure 3b), ascribed to lithium ethylene monocarbonate (4.09 and 3.59 ppm)<sup>3</sup> and ethylene glycol (3.40 ppm).<sup>40</sup> The reaction of EC with 100 mM potassium superoxide after 24 h also produces LEMC and EG, more than was observed for the reaction with peroxide, but also yields multiple additional signals (Figure 3a); the <sup>1</sup>H NMR spectrum shows the presence of the formate anion (8.58 ppm), formic acid (8.18 ppm), a poly(ethylene oxide)-like species (3.69 and 3.40 ppm), as well as signals tentatively assigned to potassium formate (8.21 ppm) and the peroxide-derivative of ethylene monocarbonate/potassium ethylene monocarbonate (4.13 and 3.81 ppm).<sup>41,42</sup> No hydrogen peroxide was detected (~10.6 ppm; Figure 3a), suggesting minimal disproportionation of the lithium peroxide salt.

Analogous <sup>1</sup>H NMR results were obtained for the reaction between PC and potassium superoxide (Figure S14). The presence of a formate species is consistent with that previously reported to form in Li–O<sub>2</sub> cells using a PC-based electrolyte. <sup>21</sup> The evolution of reaction products was slower, consistent with the slower gas evolution observed for PC (Figure 2).

Linear Alkyl Carbonates. The <sup>1</sup>H NMR spectra for DMC, EMC and DEC after reaction with the three ROS show the formation of similar products, where differences in observed products are consistent with the variations in alkyl chain lengths of the carbonates. For clarity and ease of assignment, the following analysis focuses on the DMC reaction mixtures, as DMC itself only yields a single NMR signal, compared to three for EMC and two for DEC. The <sup>1</sup>H NMR spectra for the reactions with EMC and DEC are shown in the Supporting Information (Figures S15 and S16).

The <sup>1</sup>H NMR spectrum of pristine DMC shows one main signal arising from the solvent (DMC; 3.69 ppm) and two minor signals for nondeuterated DMSO and trace water (Figure 4d). The reaction of DMC with singlet oxygen yields

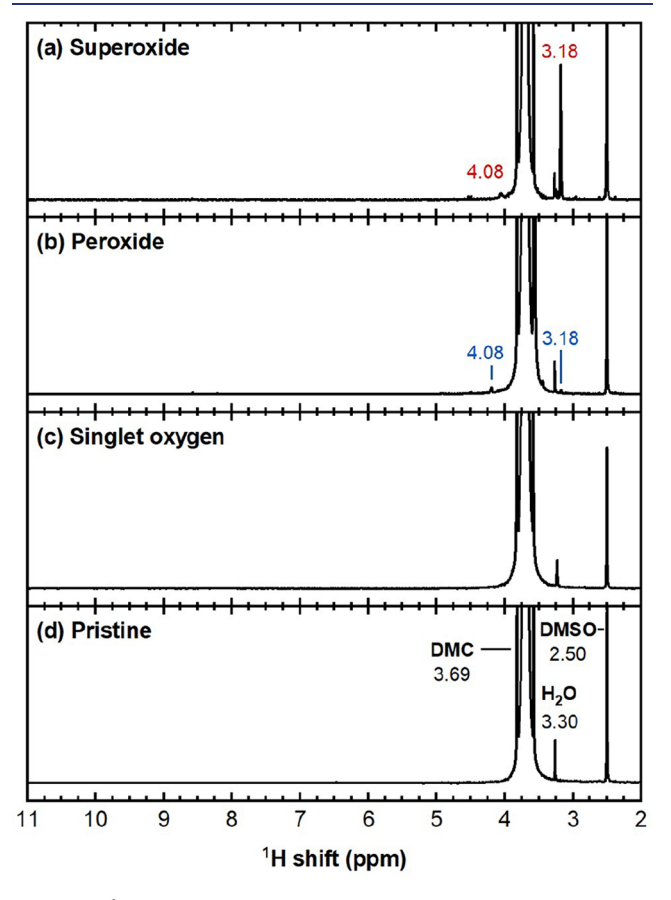


**Figure 4.** <sup>1</sup>H solution NMR spectra of dimethyl carbonate (DMC) after reaction with (a) potassium superoxide, (b) lithium peroxide, (c) singlet oxygen, and (d) pristine DMC. The signals of DMC (3.69 ppm), dimethyl sulfoxide (2.50 ppm) and residual water (3.30 ppm) are annotated in black on the bottom panel. The chemical shifts in blue and red correspond to signals that appeared after a 24 h reaction with peroxide and superoxide, respectively.

no additional signals nor an increase in the water signal (Figure 4c), consistent with previous literature and further supporting that linear carbonates are unreactive toward singlet oxygen. Similar to EC, the reaction of linear alkyl carbonates with lithium peroxide results in the formation of alcohols; the <sup>1</sup>H NMR spectrum of DMC after a 24 h reaction with lithium peroxide shows very minor formation of methanol (4.08 and 3.18 ppm; Figure 4b). Whereas the reaction of peroxide with EC led to the formation of the corresponding monocarbonate, no signal for lithium methyl carbonate (3.27 ppm) was observed, likely due to the low solubility of lithium monocarbonates in DMSO-d6. <sup>43</sup> Thus, the presence of lithium monocarbonate cannot be excluded. The reaction of DMC

with 100 mM potassium superoxide also produces methanol. Although the <sup>1</sup>H NMR signal is slightly greater than in the reaction of DMC with lithium peroxide, the overall amount remains small (Figure 4a). No signal for hydrogen peroxide (~10.6 ppm) was observed for any of the linear carbonates (Figures 4a, S15a, and S16a), further supporting that potassium superoxide does not disproportionate in these solvents. Similar results are observed for EMC and DEC, as evidenced by the formation of ethanol and its deprotonated form, (potassium) ethoxide (3.61 and 0.99 ppm), after a 24 h reaction with potassium superoxide (Figures S15a and S16a). Curiously, signals for dimethylsulfone (DMSO<sub>2</sub>; 2.98 ppm) were detected in the <sup>1</sup>H NMR spectra of all three linear alkyl carbonate samples. <sup>44,45</sup> This may form through the oxidation of the DMSO NMR solvent by potassium superoxide, 46 further implying the persistence of unreacted superoxide in the linear alkyl carbonates after 3 days. This observation, together with the H<sub>2</sub>O titration of the linear carbonate/potassium superoxide mixture (see above), provides strong evidence that linear alkyl carbonates are negligibly reactive toward potassium superoxide under the present experimental conditions.

Time Resolved Measurement of EC with  $KO_2$ . To gain further insights into these reactions, the evolution of reaction products was tracked as a function of time. 100  $\mu$ L of the reaction mixture was taken for NMR analysis at multiple time points (t=0, 2, 12, 24, 48, 72, and 96 h). The "t=0 h" sample was collected immediately after addition of  $KO_2$  to EC, with approximately 5 min elapsed before NMR data acquisition. As the gas measurements and NMR results indicate that the reaction between EC and potassium superoxide is most pronounced, the following analysis focuses on this reaction. The <sup>1</sup>H NMR spectra for the time-resolved reactions of potassium superoxide with DMC, EMC, DEC and PC are shown in the Supporting Information (Figures S17–S20).

Figure 5 shows the evolution of the <sup>1</sup>H NMR spectra of EC as it reacts with potassium superoxide over 96 h. The <sup>1</sup>H NMR signals present after 96 h correspond to the same species identified above (Figure 3a). These products are formed directly at t = 0 h, albeit in small quantities, and their signal intensities increase as the reaction continues. Water titration measurements on the reaction mixture revealed that no KO<sub>2</sub> remained after 48 h (see above), yet the intensities of the NMR signals arising from these products continue to grow beyond this point. The signals do not appear in an EC sample left for 96 h without the addition of KO<sub>2</sub> (Figure S21a), suggesting that the formation of these products indirectly involves KO2. This may also account for the continued evolution of CO<sub>2</sub> from the reaction mixture even after KO<sub>2</sub> has been consumed (Figure 1i). The water resonance observed in these spectra originates from trace water in the DMSO-d<sub>6</sub> solvent. The quantity of water, as inferred from the integral of this resonance, remains constant over the experiment; however, the signal appears reduced due to line broadening caused by dissolved O2. Thus, water is not expected to play a significant role in in the EC-KO2 reactivity.

In addition to these persistent products, the time-resolved NMR spectra also reveal the formation of transient intermediates: immediately at the start of the reaction (Figure 5b), signals assigned to glycolaldehyde (9.41 and 3.97 ppm; Figure S22a) and a second aldehyde species, possibly glyoxal (9.61 ppm), are detected; <sup>47–49</sup> however, their signals disappear within 12 h (Figure 5d). The formation of these aldehydes appears to be closely linked to the presence of KO<sub>2</sub>, as their

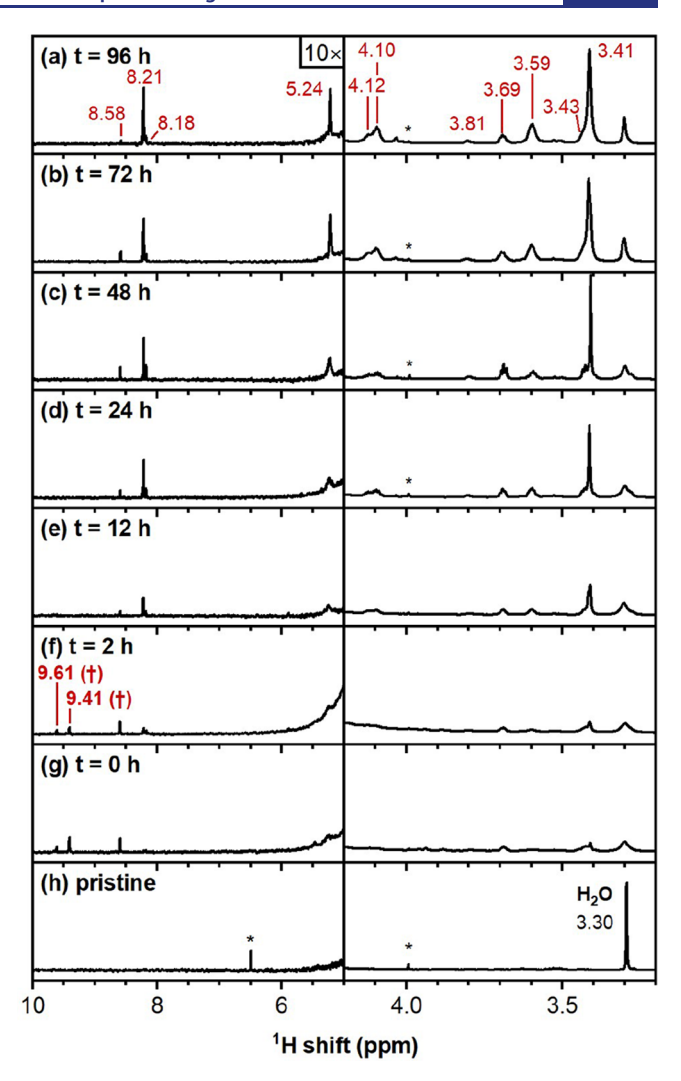


**Figure 5.** Time-resolved <sup>1</sup>H solution NMR spectra of ethylene carbonate (EC) during reaction with 100 mM potassium superoxide. NMR spectra were collected at various intervals indicated on the panels in hours. The chemical shifts in red correspond to signals that appeared during the reaction between EC and KO<sub>2</sub>. Transient species formed are indicated with a dagger (†) and impurities originating from the deuterated NMR solvent are marked with an asterisk (\*).

NMR signals are only observed while the reaction mixture is yellow (i.e., indicating the presence of  $KO_2$ ; Figure S23), and they reappear upon the addition of more  $KO_2$  after 48 h (Figure S24).

A similar, but slower, progression of product and intermediate formation was observed for PC with KO $_2$  (Figure S20). In contrast, the linear alkyl carbonates showed no time-dependent growth of product signals; instead, the respective product signals appeared immediately at t=0 and remained constant thereafter (Figures S17–S19). Notably, signals for dimethylsulfone (DMSO $_2$ ) persisted throughout the experiment in the LAC mixtures, indicating the presence of unreacted KO $_2$  in the system, available to oxidize the DMSO solvent even at extended reaction times (t=72 h).

#### DISCUSSION

Reactivity of Alkyl Carbonates with Reactive Oxygen Species. Chemical Reactivity of Singlet Oxygen, Peroxide, and Superoxide. To better understand the reactivity observed

between the alkyl carbonates and ROS, we first review the typical chemical behavior of the three ROS studied in this work. Singlet oxygen is highly electrophilic, typically reacting with alkenes, dienes and aromatics via pericyclic reactions, such as the ene reaction and cycloaddition reactions (e.g., [4+2] cycloaddition; Diels–Alder type or [2+2] cycloaddition). Singlet oxygen can also be used for hydroperoxidation of hydrocarbons and ethers, where it directly inserts into the C–H bond. 51,52

The peroxide anion is a strong oxidizer and potent nucleophile, and the hydroperoxide anion (HOO<sup>-</sup>) has been reported to be 10<sup>4</sup> as reactive as a hydroxy anion (OH<sup>-</sup>), due to the alpha effect.<sup>24,S3-55</sup> Note that reported reactions involving peroxide species describe the reactivity of the hydroperoxide anion and organic peroxides (ROO<sup>-</sup>), rather than that of the peroxide dianion.

The superoxide anion exhibits a range of reactivity, acting as a base, nucleophile, oxidizing agent, and electron transfer agent, with its exact reactivity depending on the nature of the substrate. Its dominant behavior is as a base, abstracting protons from solvents or substrates, and subsequent disproportionation to  $O_2$  and  $H_2O_2$ . Although the  $pK_a$  of superoxide is only 4.8 (typical for a weak acid) its proton abstraction ability has been reported as much greater, comparable to that of the conjugate base of an acid with a pK, of  $\sim 23.46,57$  For example, the superoxide anion fully disproportionates in an aqueous solution at pH 14,46 and can even deprotonate chloroform  $(pK_a = 15.5)^{.58}$  This strong basicity prevents superoxide from acting as a nucleophile in protic media. In aprotic media, however, superoxide behaves as powerful nucleophile: it reacts with alkyl halides via an S<sub>N</sub>2 mechanism, 46,59 and esters via attack on the carbonyl carbon, 46,60,61 yet it remains unreactive toward amides. 61,62 Additionally, superoxide can oxidize secondary alcohols to ketones and aldehydes to carboxylic acids, 63 and has been reported to participate in electron transfer reactions with transition metal complexes. 64,65

Chemical Oxidation of EC by Superoxide. Using the gaseous and soluble reaction products identified by mass spectrometry and NMR spectroscopy in this work, we propose a mechanism for the chemical oxidation of EC by superoxide. Given the basicity of superoxide, we first considered whether EC is deprotonated by superoxide (Scheme 1a). The removal of a proton yields the EC<sup>-</sup> (step I), which is speculated to then fragment into CO<sub>2</sub> and ethenolate (step II). The latter is known to be unstable and readily tautomerizes to acetaldehyde. 66 While CO<sub>2</sub> is continuously evolved during the reaction between EC and potassium superoxide, neither acetaldehyde (9.67, 2.13 ppm) or vinyl alcohol (6.45, 4.18, 3.82 ppm)<sup>66</sup> were observed in the <sup>1</sup>H NMR spectrum (Figures 3a and 5), suggesting that EC is not deprotonated by superoxide. This is supported by DFT calculations ( $\Delta G = 1.51$ ;  $\Delta G^{\ddagger} = 1.62$  eV; Figure S25; black pathway) and is consistent with previous computational studies.<sup>27</sup> This also aligns with the nucleophilic character of superoxide in aprotic media. Therefore, we propose that the decomposition of EC by superoxide via a simple deprotonation mechanism is unlikely.

Next, we explore mechanisms with superoxide acting as a nucleophile, starting with attack on the carbonyl carbon of EC (Scheme 1b; step I); this would yield a highly unstable tetrahedral intermediate, as the carbon is surrounded by 4 oxygens, which then collapses to yield the superoxide-derivative of ethylene peroxymonocarbonate (step II), which

Scheme 1. Possible Reaction Modes of the Superoxide Radical Anion with Ethylene Carbonate (EC)<sup>a</sup>

# (a) deprotonation of ethereal carbon

# (b) nucleophilic attack on carbonyl carbon

#### (c) nucleophilic attack on ethereal carbon

$$\begin{array}{c} \begin{array}{c} \begin{array}{c} \\ \\ \\ \\ \end{array} \end{array} \begin{array}{c} \begin{array}{c} \\ \\ \\ \end{array} \end{array} \begin{array}{c} \\ \\ \end{array} \begin{array}{c} \\$$

# (d) oxidation of ethylene glycol

**EMC** 

ı

EG

"Pathways (a) deprotonation and (b) nucleophilic attack at the carbonyl carbon are considered unlikely to occur based on experimental and computational results. Pathway (c), nucleophilic attack at the ethereal carbon, generates the intermediates ethylene monocarbonate (EMC) and ethylene glycol (EG), and is proposed as the dominant mechanism. Pathway (d) illustrates further oxidation of EG by superoxide.

could first quench to ethylene peroxymonocarbonate through a second equivalent of superoxide (step III) and eventually to ethylene monocarbonate through a second EC molecule (step IV). While ethylene monocarbonate was observed to form during the reaction between EC and potassium superoxide (Figures 3a and 5; 4.08 and 3.59 ppm), its continued formation after all potassium superoxide has been consumed (Figure 5a, t = 96 h), suggests that it is not formed directly by attack of the superoxide anion into the carbonyl carbon of EC. This is supported by DFT calculations, which show that nucleophilic attack by the superoxide radical anion at the carbonyl carbon of EC is thermodynamically unfavorable ( $\Delta G = 1.97$ ;  $\Delta G^{\ddagger} = 2.50$  eV; Figure S25; blue pathway). This is also consistent with the low electrophilicity of the carbonate

carbon, akin to that in amides, which are known to be unreactive toward superoxide. Thus, EC is unlikely to react with superoxide via direct nucleophilic attack on the carbonyl carbon.

Instead, we propose that superoxide reacts with EC through nucleophilic attack on the ethereal carbon of EC (Scheme 1c; step I), yielding a different superoxide-derivative of ethylene monocarbonate as discussed above. This pathway is supported by DFT calculations, indicating that the reaction is both thermodynamically and kinetically favorable ( $\Delta G = -0.31$ ;  $\Delta G^{\ddagger}$  = 0.74 eV; Figure S25; red pathway). This is also consistent with previous DFT calculations performed on both EC and PC, indicating that attack at the ethereal carbon is favorable. 21,27 This proposed mechanism is also consistent with the observation of m/z = 77 fragments, attributed to the decarbonated peroxide-derivative of ethylene carbonate—in acid titrations of cycled cathodes known to release ROS.67 Consistent with mechanisms reported for esters, we suggest that this organic superoxide derivative could then be quenched by a second equivalent of superoxide (step II), yielding O<sub>2</sub> (gas) and the peroxide derivative of ethylene monocarbonate (step III). The peroxide derivative may then react with another equivalent of EC to give two equivalents of ethylene monocarbonate, which can decarboxylate to form ethylene glycol and CO2 (step IV). This mechanism would be consistent with the formation of CO<sub>2</sub> and O<sub>2</sub> confirmed by mass spectrometry, as well as the observation of ethylene glycol (3.41 ppm), ethylene monocarbonate (4.08 and 3.59 ppm) and possible the peroxide derivative of ethylene monocarbonate (4.13 and 3.81 ppm) in the <sup>1</sup>H NMR spectra of EC + KO<sub>2</sub> (Figures 3a and 5). As shown by the KO<sub>2</sub> concentrationdependence experiments (Figure S5), the CO<sub>2</sub> evolution rate per mole of KO<sub>2</sub> is comparable across concentrations, consistent with a first-order process. This suggests that the decomposition of ethylene monocarbonate to CO<sub>2</sub> and ethylene glycol is the rate-determining step for CO<sub>2</sub> evolution.

The ethylene glycol could be oxidized further by superoxide to generate CO<sub>2</sub> as the final product. Glycolaldehyde (9.41 and 3.97 ppm) and glyoxal (9.61 ppm) are both well-known intermediates in the oxidation of ethylene glycol,<sup>47</sup> and are observed as transient species in the reaction between EC and potassium superoxide. While this reaction is demonstrated for ethylene glycol in Scheme 1d, this oxidation may not need to occur sequentially and could possibly proceed via a concerted reaction from the peroxide, or even the superoxide intermediates.

Finally, the continued  $CO_2$  evolution observed well after the potassium superoxide has been consumed (i.e., beyond 96 h, compared to complete  $KO_2$  consumption in less than 12 h) may result from the hydrolysis of EC by other reactive oxygen species formed in reactions outlined above or through reactions with any protic impurities (e.g.,  $OH^-$ ,  $ROO^-$ ,  $HOO^-$ , etc.). This continued  $CO_2$  evolution complicates establishing the overall stoichiometry of the reaction between EC and  $KO_2$ .

The reaction between EC and the more stable (lithium) peroxide is expected to occur via a similar mechanism, however the higher activation energy may account for the limited reactivity that is observed. In the case of singlet oxygen, its short lifetime in solution  $(\sim 10^{-6} \text{ s})^{38}$  also contributes, at least in part, to the limited reactivity observed.

Reactivity with Linear Alkyl Carbonates. The gas evolution and NMR results in this work suggest that the linear alkyl

carbonates (DMC, EMC, and DEC) exhibit markedly lower reactivity toward reactive oxygen species than cyclic alkyl carbonates under the present experimental conditions.

One possible explanation for this observed lack of reactivity is the poor solubility of ionic species in the linear alkyl carbonates. The dielectric constants of DMC ( $\varepsilon = 3.1$ ), EMC ( $\varepsilon$  = 2.9) and DEC ( $\varepsilon$  = 2.8) are an order of magnitude lower than that of EC ( $\varepsilon$  = 90), reflecting their significantly lower polarity and reduced ability to stabilize charged intermediates.<sup>32</sup> Even with the addition of crown ether to enhance the solubility of potassium superoxide and lithium peroxide, negligible reactivity was observed: no CO2 evolution was detected (Figure S4), <sup>1</sup>H NMR spectra revealed only trace amounts of alcohols, and H2O titrations indicated that most superoxide remained unreacted. These results suggest that, even when solubilized, superoxide and peroxide species are unreactive toward linear alkyl carbonates, and that the lack of reactivity is not due to solubility limitations. Moreover, PC ( $\varepsilon$ = 65) has a higher dielectric constant than an equal-volume mixture of EC and DMC ( $\varepsilon = 30$ ), yet gas evolution for PC is an order of magnitude lower, further suggesting that the absence of reactivity for the linear alkyl carbonates is not (solely) due to solubility effects. Overall, these results suggest that linear alkyl carbonates are inherently more resistant to decomposition by reactive oxygen species.

To further investigate the origin of the reduced reactivity of linear alkyl carbonates, we performed DFT calculations for DMC, as a representative solvent, using the same approach as for EC. In the case of DMC, which has a lower dielectric constant than EC and is generally considered a worse solvent for salt dissociation compared to EC, <sup>68</sup> KO<sub>2</sub> is not expected to undergo significant ion pair separation. When the potassium counterion remains closely associated with the superoxide anion, the overall reaction pathway is kinetically limited (Figures S27 and S28), in contrast to the favorable energetics calculated for EC, where ion separation is more feasible. These computational results are consistent with our experimental observations of no detectable CO<sub>2</sub> or O<sub>2</sub> evolution and support the conclusion that reduced ion solvation in linear alkyl carbonates suppress their chemical oxidation by KO<sub>2</sub>.

Implications for Lithium-Ion and Sodium-Ion Bat**teries.** The findings of this work may be relevant for batteries employing positive electrode materials that undergo oxygen redox, such as Li-rich layered and disordered transition metal oxides, as this process is known to generate reactive oxygen species. 1,69-71 Our results indicate that EC is significantly more reactive than the linear alkyl carbonates toward these reactive oxygen species, suggesting that reducing the EC content in electrolyte solutions could help mitigate electrolyte decomposition reactions. Previous studies have already reported improved electrochemical performance with EC-lean and ECfree electrolytes; 72-77 our findings may provide a mechanistic explanation for these improvements. In parallel, the identification and development of alternative, ROS-stable solvents that can replace EC, while maintaining essential properties (e.g., ionic conductivity, SEI formation), will be critical. Similarly, these findings may help explain the poor performance of alkali metal-oxygen batteries employing carbonatebased electrolyte solutions, 20-23 as these battery systems obviously exclusively rely on oxygen redox. Overall, these insights on the reactivity of alkyl carbonates with reactive oxygen species may be used to inform the development of electrolyte solutions for next-generation cathode materials that rely on oxygen redox.

In a full cell-environment, the acidic and protic species identified here (e.g., formic acid, methanol) could migrate from the positive electrode to the negative electrode and be reduced (to, e.g., lithium formate or lithium methoxide) or react with SEI components (e.g., Li<sub>2</sub>CO<sub>3</sub>), possibly compromising the stability and passivation qualities of the SEI. While the present study focuses on the isolated chemical reactivity of carbonate solvent with ROS, these cross-talk processes represent an important potential degradation pathway in practical cells and warrant further investigation.

Altogether, these insights on the reactivity of alkyl carbonates with reactive oxygen species may be used to inform the development of electrolyte solutions for next-generation cathode materials that rely on oxygen redox. Furthermore, our findings may guide the rational design of novel cathode materials; strategies such as tuning transition metal composition, lithium content, or doping, could be used to suppress the superoxide-character of lattice oxygen, with the hope of facilitating their practical implementation.

#### CONCLUSIONS

This work focused on exploring the reactivity between commonly used alkyl carbonate battery solvents and reactive oxygen species. A combination of mass spectrometry and NMR spectroscopy was used to establish the presence of a reaction, and to identify reaction products arising from the reactions between the alkyl carbonates (EC, DMC, EMC, and DEC) and the reactive oxygen species: singlet oxygen, peroxide and superoxide. EC was found to be reactive toward all three reactive oxygen species, with the highest reactivity observed for superoxide, followed by peroxide and singlet oxygen. Linear alkyl carbonates were found to show minimal reactivity toward ROS under the conditions used in this work. Although limited solubility of lithium peroxide and potassium superoxide may contribute to this lack of reactivity, the addition of a crown ether to enhance solubility still resulted in minimal reaction. These experimental results suggest that linear alkyl carbonates possess an inherent stability against reactive oxygen species. Complementary DFT calculations further support the proposed mechanism for EC oxidation by superoxide, providing additional insight into the reaction pathway. The insights gained in this work may guide the development of new electrolyte formations, particularly for battery systems that rely on oxygen redox and thus generate reactive oxygen species.

## ASSOCIATED CONTENT

#### Supporting Information

The Supporting Information is available free of charge at https://pubs.acs.org/doi/10.1021/jacs.5c12089.

Experimental details for singlet oxygen, peroxide, and superoxide reactivity measurements; additional gas evolution data with crown ethers; isotopic labeling experiments; supplementary NMR spectra and product assignments; time-resolved NMR data for all carbonate solvents; DFT computational details and energy diagrams; and supplementary figures and tables referenced in the main text (PDF)

#### AUTHOR INFORMATION

#### **Corresponding Author**

Bryan D. McCloskey — Energy Storage and Distributed Resources Division, Lawrence Berkeley National Laboratory, Berkeley, California 94720, United States; Department of Chemical and Biomolecular Engineering, University of California — Berkeley, Berkeley, California 94720, United States; orcid.org/0000-0001-6599-2336; Email: bmcclosk@berkeley.edu

#### **Authors**

Bernardine L. D. Rinkel – Energy Storage and Distributed Resources Division, Lawrence Berkeley National Laboratory, Berkeley, California 94720, United States; Department of Chemical and Biomolecular Engineering, University of California – Berkeley, Berkeley, California 94720, United States; orcid.org/0000-0003-4455-7313

Rohith Srinivaas Mohanakrishnan — Department of Materials Science and Engineering, University of California — Berkeley, Berkeley, California 94720, United States; Materials Science Division, Lawrence Berkeley National Laboratory, Berkeley, California 94720, United States; orcid.org/0000-0003-1898-0660

Jaeheon Lee — Energy Storage and Distributed Resources Division, Lawrence Berkeley National Laboratory, Berkeley, California 94720, United States; Department of Chemical and Biomolecular Engineering, University of California — Berkeley, Berkeley, California 94720, United States;

ocid.org/0000-0002-9285-0728

Kristin A. Persson — Department of Materials Science and Engineering, University of California — Berkeley, Berkeley, California 94720, United States; Materials Science Division, Lawrence Berkeley National Laboratory, Berkeley, California 94720, United States; © orcid.org/0000-0003-2495-5509

Complete contact information is available at: https://pubs.acs.org/10.1021/jacs.5c12089

#### Notes

The authors declare no competing financial interest.

# ACKNOWLEDGMENTS

This research was supported by the Assistant Secretary for Energy Efficiency and Renewable Energy, Office of Vehicle Technologies of the U.S. Department of Energy under Contract DE-AC02-05CH11231 through the Disordered Rocksalt (DRX+) Program. The authors thank Drs. Hasan Celik, Raynald Giovine, and Pines Magnetic Resonance Center's Core NMR Facility (PMRC Core) for spectroscopic assistance. The instrument used in this work was in part supported by NIH S10OD024998.

#### REFERENCES

- (1) Jung, R.; Metzger, M.; Maglia, F.; Stinner, C.; Gasteiger, H. A. Oxygen Release and Its Effect on the Cycling Stability of LiNi x Mn y Co z O 2 (NMC) Cathode Materials for Li-Ion Batteries. *J. Electrochem. Soc.* **2017**, *164* (7), A1361–A1377.
- (2) Jung, R.; Metzger, M.; Maglia, F.; Stinner, C.; Gasteiger, H. A. Chemical versus Electrochemical Electrolyte Oxidation on NMC111, NMC622, NMC811, LNMO, and Conductive Carbon. *J. Phys. Chem. Lett.* **2017**, *8* (19), 4820–4825.
- (3) Rinkel, B. L. D.; Hall, D. S.; Temprano, I.; Grey, C. P. Electrolyte Oxidation Pathways in Lithium-Ion Batteries. *J. Am. Chem. Soc.* **2020**, 142 (35), 15058–15074.

- (4) Rinkel, B. L. D.; Vivek, J. P.; Garcia-Araez, N.; Grey, C. P. Two Electrolyte Decomposition Pathways at Nickel-Rich Cathode Surfaces in Lithium-Ion Batteries. *Energy Environ. Sci.* **2022**, *15* (8), 3416–3438.
- (5) Aurbach, D.; Gamolsky, K.; Markovsky, B.; Salitra, G.; Gofer, Y.; Heider, U.; Oesten, R.; Schmidt, M. The Study of Surface Phenomena Related to Electrochemical Lithium into LixMOy Host Materials (M = Ni, Mn). *J. Electrochem. Soc.* **2000**, *147* (4), 1322–1331.
- (6) Xing, L.; Li, W.; Wang, C.; Gu, F.; Xu, M.; Tan, C.; Yi, J. Theoretical Investigations on Oxidative Stability of Solvents and Oxidative Decomposition Mechanism of Ethylene Carbonate for Lithium Ion Battery Use. *J. Phys. Chem. B* **2009**, *113* (52), 16596–16602.
- (7) Tebbe, J. L.; Fuerst, T. F.; Musgrave, C. B. Degradation of Ethylene Carbonate Electrolytes of Lithium Ion Batteries via Ring Opening Activated by LiCoO2 Cathode Surfaces and Electrolyte Species. ACS Appl. Mater. Interfaces 2016, 8 (40), 26664–26674.
- (8) Wandt, J.; Freiberg, A. T. S.; Ogrodnik, A.; Gasteiger, H. A. Singlet Oxygen Evolution from Layered Transition Metal Oxide Cathode Materials and Its Implications for Lithium-Ion Batteries. *Mater. Today* **2018**, 21 (8), 825–833.
- (9) Papp, J. K.; Li, N.; Kaufman, L. A.; Naylor, A. J.; Younesi, R.; Tong, W.; McCloskey, B. D. A Comparison of High Voltage Outgassing of LiCoO2, LiNiO2, and Li2MnO3 Layered Li-Ion Cathode Materials. *Electrochim. Acta* **2021**, *368*, No. 137505.
- (10) Renfrew, S. E.; McCloskey, B. D. Residual Lithium Carbonate Predominantly Accounts for First Cycle CO2 and CO Outgassing of Li-Stoichiometric and Li-Rich Layered Transition-Metal Oxides. *J. Am. Chem. Soc.* **2017**, *139* (49), 17853–17860.
- (11) Ramakrishnan, S.; Park, B.; Wu, J.; Yang, W.; McCloskey, B. D. Extended Interfacial Stability through Simple Acid Rinsing in a Li-Rich Oxide Cathode Material. *J. Am. Chem. Soc.* **2020**, *142* (18), 8522–8531.
- (12) Crafton, M. J.; Huang, T.-Y.; Cai, Z.; Konz, Z. M.; Guo, N.; Tong, W.; Ceder, G.; McCloskey, B. D. Dialing in the Voltage Window: Reconciling Interfacial Degradation and Performance Decay for Cation-Disordered Rocksalt Cathodes. *J. Electrochem. Soc.* **2024**, 171 (2), No. 020530.
- (13) Huang, T. Y.; Cai, Z.; Crafton, M. J.; Giovine, R.; Patterson, A.; Hau, H. M.; Rastinejad, J.; Rinkel, B. L. D.; Clément, R. J.; Ceder, G.; McCloskey, B. D. Chemical Origin of in Situ Carbon Dioxide Outgassing from a Cation-Disordered Rock Salt Cathode. *Chem. Mater.* **2024**, *36* (13), 6535–6546.
- (14) Moshkovich, M.; Cojocaru, M.; Gottlieb, H. E.; Aurbach, D. The Study of the Anodic Stability of Alkyl Carbonate Solutions by in Situ FTIR Spectroscopy, EQCM, NMR and MS. *J. Electroanal. Chem.* **2001**, *497*, 84–96.
- (15) Zhang, X.; Kostecki, R.; Richardson, T. J.; Pugh, J. K.; Ross, P. N. Electrochemical and Infrared Studies of the Reduction of Organic Carbonates. *J. Electrochem. Soc.* **2001**, *148* (12), A1341.
- (16) Al-Nu'airat, J.; Oluwoye, I.; Zeinali, N.; Altarawneh, M.; Dlugogorski, B. Z. Review of Chemical Reactivity of Singlet Oxygen with Organic Fuels and Contaminants. *Chem. Rec.* **2021**, *21* (2), 315–342.
- (17) Clennan, E. L. New Mechanistic and Synthetic Aspects of Singlet Oxygen Chemistry. *Tetrahedron* **2000**, *56*, 9151–9179.
- (18) McCalla, E.; Abakumov, A. M.; Saubanere, M.; Foix, D.; Berg, E. J.; Rouse, G.; Doublet, M.-L.; Gonbeau, D.; Novak, P.; Van Tendeloo, G.; Dominko, R.; Tarascon, J.-M. Visualization of O-O Peroxo-like dimers in High-Capacity Layered for Li-Ion Batteries. *Science* 1979, 350 (6267), 1516—1521.
- (19) Genreith-Schriever, A. R.; Banerjee, H.; Menon, A. S.; Bassey, E. N.; Piper, L. F. J.; Grey, C. P.; Morris, A. J. Oxygen Hole Formation Controls Stability in LiNiO2 Cathodes. *Joule* **2023**, *7* (7), 1623–1640.
- (20) McCloskey, B. D.; Bethune, D. S.; Shelby, R. M.; Girishkumar, G.; Luntz, A. C. Solvents Critical Role in Nonaqueous Lithium-Oxygen Battery Electrochemistry. *J. Phys. Chem. Lett.* **2011**, 2 (10), 1161–1166.

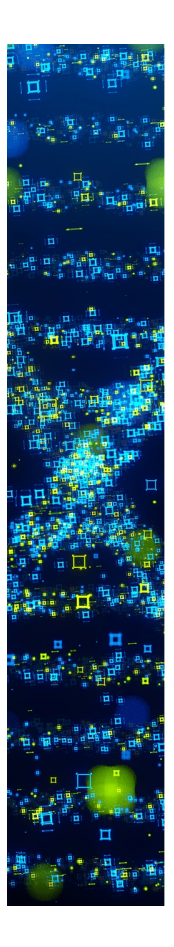
- (21) Freunberger, S. A.; Chen, Y.; Peng, Z.; Griffin, J. M.; Hardwick, L. J.; Bardé, F.; Novák, P.; Bruce, P. G. Reactions in the Rechargeable Lithium-O2 Battery with Alkyl Carbonate Electrolytes. *J. Am. Chem. Soc.* **2011**, *133* (20), 8040–8047.
- (22) Xu, W.; Viswanathan, V. V.; Wang, D.; Towne, S. A.; Xiao, J.; Nie, Z.; Hu, D.; Zhang, J. G. Investigation on the Charging Process of Li2O2-Based Air Electrodes in Li-O2 Batteries with Organic Carbonate Electrolytes. *J. Power Sources* **2011**, *196* (8), 3894–3899.
- (23) Mizuno, F.; Nakanishi, S.; Kotani, Y.; Yokoishi, S.; Iba, H. Rechargeable Li-Air Batteries with Carbonate-Based Liquid Electrolytes. *Electrochemistry* **2010**, 78 (5), 403–405.
- (24) Laino, T.; Curioni, A. A New Piece in the Puzzle of Lithium/ Air Batteries: Computational Study on the Chemical Stability of Propylene Carbonate in the Presence of Lithium Peroxide. *Chem. Eur. J.* **2012**, *18* (12), 3510–3520.
- (25) Bryantsev, V. S.; Blanco, M. Computational Study of the Mechanisms of Superoxide-Induced Decomposition of Organic Carbonate-Based Electrolytes. *J. Phys. Chem. Lett.* **2011**, 2 (5), 379–383.
- (26) Freiberg, A. T. S.; Roos, M. K.; Wandt, J.; De Vivie-Riedle, R.; Gasteiger, H. A. Singlet Oxygen Reactivity with Carbonate Solvents Used for Li-Ion Battery Electrolytes. *J. Phys. Chem. A* **2018**, *122* (45), 8828–8839.
- (27) Spotte-Smith, E. W. C.; Vijay, S.; Petrocelli, T. B.; Rinkel, B. L. D.; McCloskey, B. D.; Persson, K. A. A Critical Analysis of Chemical and Electrochemical Oxidation Mechanisms in Li-Ion Batteries. *J. Phys. Chem. Lett.* **2024**, *15* (2), 391–400.
- (28) Gottschalk, P.; Paczkowski, J.; Neckers, D. C. Factors Influencing the Quantum Yields for Rose Bengal Formation of Singlet Oxygen. *J. Photochem.* **1986**, *35* (3), 277–281.
- (29) Huang, T. Y.; Crafton, M. J.; Yue, Y.; Tong, W.; McCloskey, B. D. Deconvolution of Intermixed Redox Processes in Ni-Based Cation-Disordered Li-Excess Cathodes. *Energy Environ. Sci.* **2021**, *14* (3), 1553–1562.
- (30) Mccloskey, B. D.; Valery, A.; Luntz, A. C.; Gowda, S. R.; Wallraff, G. M.; Garcia, J. M.; Mori, T.; Krupp, L. E. Combining Accurate O2 and Li2O2 Assays to Separate Discharge and Charge Stability Limitations in Nonaqueous Li-O 2 Batteries. *J. Phys. Chem. Lett.* 2013, 4 (17), 2989–2993.
- (31) Wu, X.; Sun, Q.; Pu, Z.; Zheng, T.; Ma, W.; Yan, W.; Xia, Y.; Wu, Z.; Huo, M.; Li, X.; Ren, W.; Gong, S.; Zhang, Y.; Gao, W. Enhancing GPU-Acceleration in the Python-Based Simulations of Chemistry Frameworks. *Wiley Interdiscip. Rev.: Comput. Mol. Sci.* 2025, 15 (2), No. e70008.
- (32) Hall, D. S.; Self, J.; Dahn, J. R. Dielectric Constants for Quantum Chemistry and Li-Ion Batteries: Solvent Blends of Ethylene Carbonate and Ethyl Methyl Carbonate. *J. Phys. Chem. C* **2015**, *119* (39), 22322–22330.
- (33) Read, J.; Mutolo, K.; Ervin, M.; Behl, W.; Wolfenstine, J.; Driedger, A.; Foster, D. Oxygen Transport Properties of Organic Electrolytes and Performance of Lithium/Oxygen Battery. *J. Electrochem. Soc.* **2003**, *150* (10), A1351.
- (34) Mahne, N.; Schafzahl, B.; Leypold, C.; Leypold, M.; Grumm, S.; Leitgeb, A.; Strohmeier, G. A.; Wilkening, M.; Fontaine, O.; Kramer, D.; Slugovc, C.; Borisov, S. M.; Freunberger, S. A. Singlet Oxygen Generation as a Major Cause for Parasitic Reactions during Cycling of Aprotic Lithium-Oxygen Batteries. *Nat. Energy* **2017**, *2* (5), 1–9.
- (35) Dougassa, Y. R.; Jacquemin, J.; El Ouatani, L.; Tessier, C.; Anouti, M. Viscosity and Carbon Dioxide Solubility for LiPF6, LiTFSI, and LiFAP in Alkyl Carbonates: Lithium Salt Nature and Concentration Effect. *J. Phys. Chem. B* **2014**, *118* (14), 3973–3980. (36) Mourad, E.; Petit, Y. K.; Spezia, R.; Samojlov, A.; Summa, F. F.;
- (36) Mourad, E.; Petit, Y. K.; Spezia, R.; Samojlov, A.; Summa, F. F.; Prehal, C.; Leypold, C.; Mahne, N.; Slugovc, C.; Fontaine, O.; Brutti, S.; Freunberger, S. A. Singlet Oxygen from Cation Driven Superoxide Disproportionation and Consequences for Aprotic Metal-O2 Batteries. *Energy Environ. Sci.* **2019**, *12* (8), 2559–2568.

- (37) Dong, S.; Yang, S.; Chen, Y.; Kuss, C.; Cui, G.; Johnson, L. R.; Gao, X.; Bruce, P. G. Singlet Oxygen and Dioxygen Bond Cleavage in the Aprotic Lithium-Oxygen Battery. *Joule* **2022**, *6* (1), 185–192.
- (38) Wilkinson, F.; Helman, W. P.; Ross, A. B. Rate Constants for the Decay and Reactions of the Lowest Electronically Excited Singlet State of Molecular Oxygen in Solution. *An Expanded and Revised Compilation. J. Phys. Chem. Ref Data* 1995, 24 (2), 663–677.
- (39) Fulmer, G. R.; Miller, A. J. M.; Sherden, N. H.; Gottlieb, H. E.; Nudelman, A.; Stoltz, B. M.; Bercaw, J. E.; Goldberg, K. I. NMR Chemical Shifts of Trace Impurities: Common Laboratory Solvents, Organics, and Gases in Deuterated Solvents Relevant to the Organometallic Chemist. *Organometallics* **2010**, *29* (9), 2176–2179.
- (40) Gottlieb, H. E.; Kotlyar, V.; Nudelman, A. NMR Chemical Shifts of Common Laboratory Solvents as Trace Impurities. *J. Org. Chem.* 1997, 62, 7512–7515.
- (41) Shen, Q.; Cao, C.; Huang, R.; Zhu, L.; Zhou, X.; Zhang, Q.; Gu, L.; Song, W. Single Chromium Atoms Supported on Titanium Dioxide Nanoparticles for Synergic Catalytic Methane Conversion under Mild Conditions. *Angewandte Chemie International Edition* **2020**, 59 (3), 1216–1219.
- (42) Hu, Z.; Cheng, X.; Chen, S.; Zhu, Q.; Chen, W.; Xu, Q.; Liu, B.; He, Y.; Xing, L.; Truhlar, D. G.; Wang, Z. Unraveling Chain Branching in Cool Flames. *J. Am. Chem. Soc.* **2024**, *146*, 28060–28069.
- (43) Xu, K.; Zhuang, G. V.; Allen, J. L.; Lee, U.; Zhang, S. S.; Ross, P. N.; Jow, T. R. Syntheses and Characterization of Lithium Alkyl Mono- and Bicarbonates as Components of Surface Films in Li-Ion Batteries. *J. Phys. Chem. B* **2006**, *110* (15), 7708–7719.
- (44) Yamada, Y.; Teoh, C. M.; Toyoda, Y.; Tanaka, K. Direct Catalytic Benzene Hydroxylation under Mild Reaction Conditions by Using a Monocationic  $\mu$ -Nitrido-Bridged Iron Phthalocyanine Dimer with 16 Peripheral Methyl Groups. *New J. Chem.* **2022**, 46 (3), 955–958.
- (45) Jereb, M. Highly Atom-Economic, Catalyst- and Solvent-Free Oxidation of Sulfides into Sulfones Using 30% Aqueous H2O2. *Green Chem.* **2012**. *14* (11), 3047–3052.
- (46) Sawyer, D. T.; Valentine, J. S. How Super Is Superoxide? *Acc. Chem. Res.* **1981**, *14* (12), 393–400.
- (47) Chauhan, N. L.; Juvekar, V. A.; Sarkar, A. Oxidation of Ethylene Glycol: Unity of Chemical and Electrochemical Catalysis. *Electrochem. Sci. Adv.* **2022**, *2* (6), No. e2100092.
- (48) Xian, J.; Li, S.; Su, H.; Liao, P.; Wang, S.; Zhang, Y.; Yang, W.; Yang, J.; Sun, Y.; Jia, Y.; Liu, Q.; Liu, Q.; Li, G. Electrocatalytic Synthesis of Essential Amino Acids from Nitric Oxide Using Atomically Dispersed Fe on N-Doped Carbon. *Angew. Chem., Int. Ed.* **2023**, 62 (26), No. e202304007.
- (49) Bekhradnia, A. R.; Arshadi, S. Efficient Selective Oxidation of Organic Substrates Using Pyridinum Sulfonate Halochromate under Solvent-Free Conditions and Microwave Irradiation: Experimental and Theoretical Study. Synthesis and Reactivity in Inorganic, Metal-Organic and Nano-Metal Chemistry 2012, 42 (5), 705–710.
- (50) You, Y. Chemical Tools for the Generation and Detection of Singlet Oxygen. Org. Biomol Chem. 2018, 16 (22), 4044-4060.
- (51) Sagadevan, A.; Hwang, K. C.; Su, M. D. Singlet Oxygen-Mediated Selective C-H Bond Hydroperoxidation of Ethereal Hydrocarbons. *Nat. Commun.* **2017**, *8* (1), 1812.
- (52) Yamazaki, H.; Cvetanović, R. J. Collisional Deactivation of the Excited Singlet Oxygen Atoms and Their Insertion into the CH Bonds of Propane. *J. Chem. Phys.* **1964**, *41* (12), 3703–3710.
- (53) Edwards, J. O.; Pearson, R. G. The Factors Determining Nucleophilic Reactivities. *J. Am. Chem. Soc.* **1962**, *84*, 16–24.
- (54) Klopman, G.; Tsuda, K.; Louis, J. B.; Davis, R. E. Supernucleophiles I The Alpha Effect. *Tetrahedron* **1970**, 26, 4549–4554.
- (55) Pearson, R. G.; Edgington, D. N. Nucleophilic Reactivity of the Hydrogen Peroxide Anion: Distinction Between SN2 and SN1 CB Mechanisms. *J. Am. Chem. Soc.* **1962**, *84* (23), 4607–4608.

- (56) Hayyan, M.; Hashim, M. A.; Alnashef, I. M. Superoxide Ion: Generation and Chemical Implications. *Chem. Rev.* **2016**, *116* (5), 3029–3085.
- (57) Sawyer, D. T.; Gibian, M. J. The Chemistry of Superoxide Ion. *Tetrahedron* **1979**, *35*, 1471–1481.
- (58) Purrington, S. T.; Kenion, G. B. Superoxide: Base, Nucleophile, Radical, or Electron Transfer Reagent? *J. Chem. Soc. Chem. Commun.* **1982**, *13*, 731–732.
- (59) San Filippo, J.; Chern, C.-I.; Valentine, J. S. The Reaction of Superoxide with Alkyl Halides and Tosylates. *J. Org. Chem.* **1975**, *40* (11), 1678–1680.
- (60) Gibian, M. J.; Sawyer, D. T.; Ungermann, T.; Tangpoonpholvivat, R.; Morrison, M. M. Reactivity of Superoxide Ion with Carbonyl Compounds in Aprotic Solvents. *J. Am. Chem. Soc.* 1979, 101 (3), 640–644.
- (61) San Filippo, J.; Roman, L. J.; Chern, C.-I.; Valentine, J. S. Cleavage of Esters by Super Oxide. *J. Org. Chem.* **1976**, 41 (3), 586–588.
- (62) Kornblum, N.; Singaram, S. The Conversion of Nitriles to Amides and Esters to Acids by the Action of Sodium Superoxide. *J. Org. Chem.* **1979**, *44*, 4727.
- (63) Lee-Ruff, E. The Organic Chemistry of Superoxide. Chem. Soc. Rev. 1977, 6, 195–214.
- (64) Rao, P. S.; Hayon, E. Redox Potentials of Free Radicals. IV. Superoxide and Hydroperoxy Radicals O2- and HO2. *J. Phys. Chem.* 1975, 79 (4), 397–402.
- (65) Valentine, J. S.; Quinn, A. E. Reaction of Superoxide with the Manganese(III) Tetraphenylporphine Cation. *Inorg. Chem.* **1976**, *15* (8), 1997–1999.
- (66) Capon, B.; Rycroft, D. S.; Watson, T. W.; Zucco, C. Simple Enols. I.1 The Generation of Vinyl Alcohol in Solution and Its Detection and Characterization by NMR Spectroscopy2. *J. Am. Chem. Soc.* 1981, 103, 1761–1765.
- (67) Kaufman, L. A.; McCloskey, B. D. Surface Lithium Carbonate Influences Electrolyte Degradation via Reactive Oxygen Attack in Lithium-Excess Cathode Materials. *Chem. Mater.* **2021**, 33 (11), 4170–4176.
- (68) Su, C. C.; He, M.; Amine, R.; Rojas, T.; Cheng, L.; Ngo, A. T.; Amine, K. Solvating Power Series of Electrolyte Solvents for Lithium Batteries. *Energy Environ. Sci.* **2019**, *12* (4), 1249–1254.
- (69) Huang, T. Y.; Cai, Z.; Crafton, M. J.; Kaufman, L. A.; Konz, Z. M.; Bergstrom, H. K.; Kedzie, E. A.; Hao, H. M.; Ceder, G.; McCloskey, B. D. Quantitative Decoupling of Oxygen-Redox and Manganese-Redox Voltage Hysteresis in a Cation-Disordered Rock Salt Cathode. *Adv. Energy Mater.* 2023, *13* (21), No. 2300241.
- (70) Assat, G.; Iadecola, A.; Foix, D.; Dedryvere, R.; Tarascon, J. M. Direct Quantification of Anionic Redox over Long Cycling of Li-Rich Nmc via Hard x-Ray Photoemission Spectroscopy. *ACS Energy Lett.* **2018**, 3 (11), 2721–2728.
- (71) Seo, D. H.; Lee, J.; Urban, A.; Malik, R.; Kang, S.; Ceder, G. The Structural and Chemical Origin of the Oxygen Redox Activity in Layered and Cation-Disordered Li-Excess Cathode Materials. *Nat. Chem.* **2016**, 8 (7), 692–697.
- (72) Ma, L.; Glazier, S. L.; Petibon, R.; Xia, J.; Peters, J. M.; Liu, Q.; Allen, J.; Doig, R. N. C.; Dahn, J. R. A Guide to Ethylene Carbonate-Free Electrolyte Making for Li-Ion Cells. *J. Electrochem. Soc.* **2017**, *164* (1), A5008—A5018.
- (73) Petibon, R.; Xia, J.; Ma, L.; Bauer, M. K. G.; Nelson, K. J.; Dahn, J. R. Electrolyte System for High Voltage Li-Ion Cells. *J. Electrochem. Soc.* **2016**, *163* (13), A2571–A2578.
- (74) Xia, J.; Glazier, S. L.; Petibon, R.; Dahn, J. R. Improving Linear Alkyl Carbonate Electrolytes with Electrolyte Additives. *J. Electrochem. Soc.* **2017**, *164* (6), A1239–A1250.
- (75) Petibon, R.; Harlow, J.; Le, D. B.; Dahn, J. R. The Use of Ethyl Acetate and Methyl Propanoate in Combination with Vinylene Carbonate as Ethylene Carbonate-Free Solvent Blends for Electrolytes in Li-Ion Batteries. *Electrochim. Acta* **2015**, *154*, 227–234.
- (76) Gmitter, A. J.; Plitz, I.; Amatucci, G. G. High Concentration Dinitrile, 3-Alkoxypropionitrile, and Linear Carbonate Electrolytes

Enabled by Vinylene and Monofluoroethylene Carbonate Additives. *J. Electrochem. Soc.* **2012**, *159* (4), A370–A379.

(77) Petibon, R.; Aiken, C. P.; Ma, L.; Xiong, D.; Dahn, J. R. The Use of Ethyl Acetate as a Sole Solvent in Highly Concentrated Electrolyte for Li-Ion Batteries. *Electrochim. Acta* **2015**, *154*, 287–293.



CAS BIOFINDER DISCOVERY PLATFORM™

# STOP DIGGING THROUGH DATA —START MAKING DISCOVERIES

CAS BioFinder helps you find the right biological insights in seconds

Start your search

